Biogeochemistry (2011) 103:143–158
DOI 10.1007/s10533-010-9453-2

Microbial carbon oxidation rates and pathways in sediments of two Tanzanian mangrove forests

Erik Kristensen · Perrine Mangion · Min Tang · Mogens R. Flindt · Marianne Holmer · Shadrack Ulomi

Received: 21 August 2009 / Accepted: 14 April 2010 / Published online: 6 May 2010

Abstract Temporal and spatial variations in benthic metabolism and anaerobic carbon oxidation pathways were assessed in an anthropogenically impacted (Mtoni) and a pristine (Ras Dege) mangrove forest in Tanzania. The objectives were (1) to evaluate how benthic metabolism is affected by organic carbon availability; (2) to determine the validity of diffusive release of CO_2 as a measure benthic carbon oxidation; and (3) to assess the partitioning of anaerobic carbon pathways and factors controlling the availability of electron acceptors (e.g. oxidized iron). Microbial carbon oxidation measured as diffusive exchange of O_2 and CO_2 (32–67 and 28–115 mmol m^{-2} day^{-1}, respectively) showed no specific temporal patterns. Low intertidal sediments at Mtoni fed by labile algal carbon of anthropogenic origin had higher diffusive CO_2 release than high intertidal sediments that primarily received less reactive mangrove detritus. Diffusive release of CO_2 apparently underestimated total sediment carbon oxidation due to CO_2 loss from deep sediments via emission through biogenic structures (i.e. crab burrows and pneumatophores) and porewater seepage into creeks. We propose that diffusive fluxes in the present mangrove sediments are roughly equivalent to depth-integrated reactions occurring in the upper 12 cm. Anaerobic carbon oxidation was dominated by FeR irrespective of anthropogenic influence in sediments where the oxidizing effects of biogenic structures increased the Fe(III) level. More than 80% of the anaerobic carbon oxidation in Mtoni and Ras Dege sediments was due to FeR when reactive Fe(III) exceeded 30 μmol cm^{-3}. The anthropogenic influence at Mtoni was primarily noted as up to one order of magnitude higher denitrification than at Ras Dege, but this process always accounted for less than 1% of total carbon oxidation. It is noteworthy that organic and nutrient enrichment of anthropogenic origin in Mtoni has no measurable effect on microbial processes, other than carbon oxidation in the low intertidal area and denitrification throughout the forest, and indicates a strong resilience of mangrove environments towards disturbances.

Keywords Mangrove sediment · Carbon oxidation · Electron acceptor · CO_2 flux measurement · Biogenic structures

E. Kristensen (✉) · M. R. Flindt · M. Holmer
Institute of Biology, University of Southern Denmark, 5230 Odense M, Denmark
e-mail: ebk@biology.sdu.dk

P. Mangion
Department of Analytical and Environmental Chemistry, Vrije Universiteit Brussel, Pleinlaan 2, 1050 Brussels, Belgium

M. Tang
Key Laboratory of Tropic Biological Resources of Ministry of Education, Faculty of Material and Chemical Engineering, Hainan University, 570228 Haikou, China

S. Ulomi
Faculty of Aquatic Sciences and Technology, University of Dar es Salaam, Dar es Salaam, Tanzania

Introduction

Mangrove forests are important interfaces for the transformation and exchange of organic and inorganic carbon between land, atmosphere and ocean (Borges et al. 2003; Dittmar et al. 2006; Kristensen et al. 2008a). Much of the autochthonously (tree and algal production) and allochthonously (tidal and river import) derived organic carbon reaching mangrove sediments is rapidly oxidized by the decomposer food web (Jennerjahn and Ittekkot 2002; Bouillon et al. 2008). The remainder is either exported by tides or stored permanently in the sediments.

Aerobic respiration and anaerobic sulfate reduction are usually the most important carbon oxidation pathways in mangrove sediments, with a typical share of 30–50% each (e.g. Alongi et al. 2000; Kristensen et al. 2008a). Denitrification, manganese respiration and iron respiration, on the other hand, have traditionally been considered unimportant in the carbon cycling of mature forests due to limited availability of the electron acceptors NO_3^-, Mn(IV) and Fe(III) (e.g. Alongi et al. 2000; Kristensen et al. 2000). Recent evidence suggests, however, that the role of iron respiration may be comparable to, or higher, than that of sulfate reduction in iron-rich mangrove environments (Kristensen et al. 2000; Kristensen and Alongi 2006).

Microbial carbon oxidation rates and pathways within mangrove sediments are dependent on a number of key factors. These include organic matter input, bioturbation activity, presence of tree roots and extent of tidal water cover (Middelburg et al. 1996; Berelson et al. 2002; Kitaya et al. 2002; Canfield et al. 2005; Kristensen et al. 2008b). Organic input is a key controlling factor for carbon oxidation in mangrove sediments and maintains a delicate redox balance between iron and sulfur (Ferreira et al. 2007). This balance is buffered by downward translocation of oxygen via crab burrows and tree roots, which creates sufficiently oxidized conditions to drive substantial iron respiration and prevents release of free sulfide by depressing sulfate reduction (Kristensen and Alongi 2006).

The evaluation of carbon oxidation by heterotrophic microbial communities in mangrove environments is also dependent on the approach by which sediment metabolism is measured. The release of CO_2 may in certain cases vary several fold dependent on tidal inundation with highest rates during air exposure, while in other cases there are no detectable difference (Alongi et al. 2004; Kristensen and Alongi 2006). It is not yet fully elucidated how this is controlled, but large biogenic structures (e.g. pneumatophores and crab burrows) are reported to have an important role as conduits for CO_2 release (Kristensen et al. 2008b). Also seepage of deep porewater rich in anaerobic metabolites may remove significant amounts of CO_2 (Bouillon et al. 2007; Alongi et al. 2008) rendering sediment–water and sediment–air diffusive fluxes doubtful measures of total sediment metabolism.

Anthropogenic impact through nutrient enrichment and higher organic loading may also affect the biogeochemical balance of mangrove sediments. Excess delivery of organic matter, either directly via sewage or indirectly through nutrient enrichment and eutrophication is known to affect sediment processes, promote sulfidic conditions and thus limit the recruitment and survival of flora and fauna in marine environments (Alongi et al. 2005; Granek and Ruttenberg 2008; Penha-Lopes et al. 2009). The extent by which this also occurs in mangrove environments is not fully elucidated.

In this paper, we examined benthic metabolism and anaerobic carbon oxidation pathways in sediments of the anthropogenically impacted Mtoni mangrove forest and the relatively pristine Ras Dege mangrove forest in Tanzania, Africa. Our approach was first to elucidate how microbial carbon oxidation determined from diffusive CO_2 release in mangrove sediments is affected by temporal (tidal and seasonal) and anthropogenic (nutrient and organic matter loading) disturbances. Secondly, we call attention to the apparent mismatch between diffusive sediment–water/air fluxes of CO_2 and depth integrated carbon oxidation processes. Thirdly, we assess the partitioning of anaerobic carbon oxidation pathways with emphasis on factors controlling the availability of electron acceptors, such as oxidized iron.

Materials and methods

Study area

The study was conducted in two mangrove areas affected differently by human activities, Mtoni and

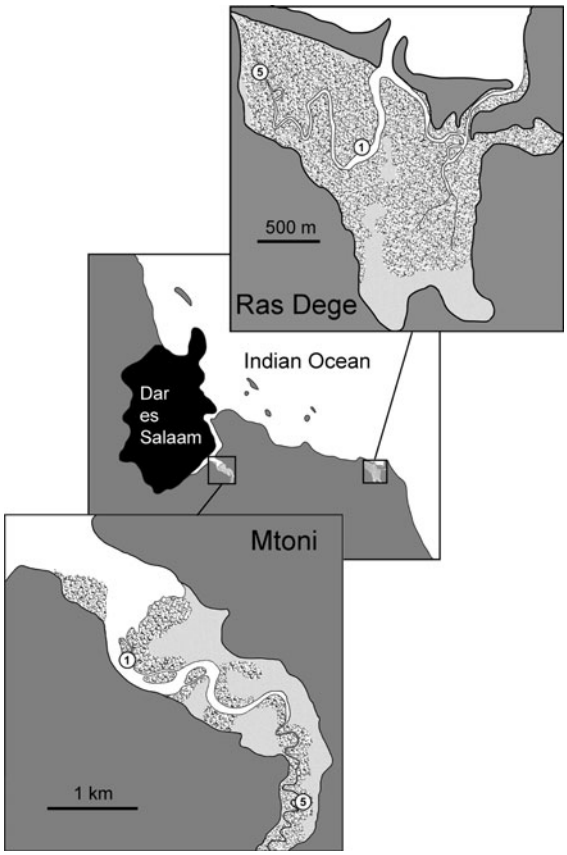

Fig. 1 Map of Mtoni and Ras Dege mangrove forests, Tanzania. *Dark grey* indicates land while *light grey* represents deforested mangrove area. The vegetated mangrove forest is hatched. Sediment sampling stations are indicated by encircled numbers

Ras Dege, near Dar es Salaam in Tanzania (Fig. 1) during sampling campaigns in September 2005 (dry season) and April 2006 (wet season). The climate in the Dar es Salaam area is humid tropical with average day and night temperatures of 28–31 and 19–25°C, respectively; warmest from October to February. The annual precipitation is about 1100 mm with two rainy (wet) seasons from March to May, and October to November.

The anthropogenically impacted Mtoni mangrove forest covers an area of about 3 km^2 and is drained by one 6 km long tidal creek, which comprises a side branch of Mzinga Creek that forms Dar es Salaam harbor. The creek receives freshwater particularly during wet seasons from streams entering at the head. There is also considerable diffuse groundwater seepage from the surrounding hills. The mangrove forest receives sewage indirectly from discharges in the harbor area and suffers severely from cutting of trees for charcoal production. The vegetation is mixed with dominance of *Sonneratia alba*, *Avicennia marina*, *Ceriops tagal* and *Rhizophora mucronata.* The shallow eutrophic area outside the mangrove forest is covered by extensive growth of drifting macroalgae that regularly enters the mangrove area by tides.

The relatively pristine Ras Dege mangrove area covers about 2 km^2, and is drained by two tidal creeks which open directly into the Indian Ocean. There are no major freshwater inputs except for surface drainage during wet seasons. Ras Dege does not receive sewage or any other wastewater discharge. It is dominated by the same tree species as Mtoni, but in different proportions due to less intense removal by felling. The mouth of the creeks and the zone adjacent to the mouth is covered by seagrass beds.

Sampling sites

Sediment fluxes, reaction rates and vertical profiles were determined about 10 m from the creek bank at two stations along the main creek at Mtoni and two stations along the western creek at Ras Dege (Fig. 1). The low intertidal Station M1 (S 06°52.760′ E 39°17.961′) at Mtoni was located near the outer boundary and the high intertidal Station M5 (S 06°53.513′ E 39°18.959′) near the upper reaches of the main creek. M1 was dominated by mature *S. alba* growing in sandy-mud sediment (143 ± 14 pneumatophores m^{-2}, Kristensen et al. 2008b), while the muddy-sand at M5 was dominated by young *C. tagal* (no pneumatophores). The low intertidal Station R1 (S 06°52.667′ E 39°27.596′) at Ras Dege was located near the outer boundary and the mid to high intertidal Station R5 (S 06°52.347′ E 39°27.169′) in the upper reaches of the forest. The sediment at R1 consisted of fine sand and the vegetation was dominated by young *A. marina* (138 ± 15 pneumatophores m^{-2}, Kristensen et al. 2008b), whereas the muddy R5 was dominated by primarily mature *R. mucronata* and few *C. tagal* (no pneumatophores). All four stations were inhabited by mixed populations of Ocypodid (primarily *Uca annulipes* and *Uca urvillei*) and Grapsid crabs (primarily *Perisesarma guttatum*) that dug numerous large burrows in the sediment (M1: 626 ± 65 m^{-2}; M5: 68 ± 17 m^{-2}; R1: 313 ± 20 m^{-2}; R5: 237 ± 53 m^{-2}, Kristensen et al. 2008b). No other large burrowing fauna (i.e. polychaetes) were observed at any station.

Sampling strategy

The spatial and temporal variation in key sediment parameters and diffusive fluxes of O_2 and CO_2 across the sediment–water/air interface was assessed from measurements at both stations in the two mangrove forests during the wet and dry seasons. Otherwise, our focus was devoted to primarily a dry season assessment of partitioning of carbon oxidation pathways in sediments at the four sampling stations. An unfortunate equipment error prevented dry season denitrification measurements and we therefore had to rely on rates obtained in the wet season only.

Sediment characteristics and porewater solutes

Triplicate sediment cores (5 cm in diameter) were taken from each station for determination of sediment characteristics and porewater solutes. Cores were analyzed for water content, wet density, particulate organic carbon (POC) and nitrogen (PON), Chlorophyll *a* (Chl. *a*) and porewater SO_4^{2-} and Cl^- during both seasons, while analysis of grain size distribution and solid phase Fe were conducted only in the dry season. Cores were in the laboratory sliced into the following depth intervals: 0–1, 1–2, 2–3, 3–4, 4–6, 6–8 and 10–12 cm before any further handling. The results are presented as pooled values for 0–4 and 4–12 cm, except for Chl. *a*, solid phase Fe and porewater solutes.

Water content was determined from water loss upon drying of sediment subsamples at 100°C for 24 h. Wet density was measured as the weight of a known sediment volume. The dried sediments were subsequently used for determination of POC and PON by a Carlo Erba model EA1108 CHNS analyzer using the difference-on-ignition method (Kristensen and Andersen 1987). Sediment grain size distribution (dry weight) at each station was obtained from wet sieving of sediment through a standard Wentworth series of sieves (1000, 500, 250, 125 and 63 μm). Solid phase Fe was extracted by a modified version of the HCl technique of Lovley and Phillips (1987). Briefly, 100–300 mg subsamples were extracted in 5 ml of 0.5 M HCl for 30 min on a shaking platform. After centrifugation ($400\times g$) for 10 min, 50 μl of the supernatant was transferred to 2 ml Ferrozine solution for Fe(II) analysis and to 2 ml Ferrozine solution containing the reducing agent hydroxylamine ($10\ g\ l^{-1}$) for total-Fe (Fe(II) + Fe(III)) analysis. The reactive amorphous Fe(III) oxide concentration was then operationally defined as the difference between total Fe and Fe(II) (Kostka and Luther 1994). Chl *a* content was analyzed by the standard spectrophotometric method (Parsons et al. 1984) on the 0–1 cm slice only. Subsamples of sediment were extracted overnight in 5 ml of 90% ethanol in darkness at 5°C. The extract was centrifuged at 3000 rpm and absorbance of the supernatant was measured at 665 and 750 nm before and after acidification.

Porewater was extracted by transferring sediment slices to 50-ml tubes followed by centrifugation at $1200\times g$ for 10 min. The supernatant porewater was GF/F filtered, acidified (pH <3) and analyzed for SO_4^{2-} and Cl^- by ion chromatography with a Dionex autosuppressed anion system (IonPac AS4A-SC column and ASRS suppressor).

Diffusive sediment–water exchange of O_2 and CO_2

Diffusive exchange of O_2 and total CO_2 (i.e. $CO_3^{2-} + HCO_3^- + CO_2$) across the sediment–water interface (diffusive S–W) in darkness was determined in the laboratory by the core-incubation technique. Triplicate sediment cores (8 cm diameter and 20 cm long) without any visible biogenic structures (large burrow openings and pneumatophores) were carefully collected at the sampling stations during low tide. The air-exposed cores were transported to the laboratory and immediately submerged in tanks containing creek water from the sampling sites, such that the water surface was at least 2 cm above the upper edge of the core liners. The water column inside the core tubes was about 10 cm. Cores were maintained in the dark overnight under continuous aeration before initiating flux measurements. Water temperature was kept constant at 27–29°C and salinity varied from 2 to 45 depending on season and station.

The cores were sealed gas tight with a removable lid and kept in darkness during flux incubations. A magnetic stirrer driven by an external rotating magnet (60 rpm) maintained a continuous water circulation at a rate well below the resuspension limit. Water samples for O_2 and total CO_2 were taken from the water phase inside each core at the start (before

inserting lids) and end (after removing lids) of 3–5 h incubation periods.

O_2 was analyzed immediately using the standard Winkler technique (Parsons et al. 1984). Samples for total CO_2 analysis were preserved with $HgCl_2$ and analyzed as soon as possible using the flow injection/diffusion cell technique of Hall and Aller (1992).

Diffusive sediment–air exchange of O_2 and CO_2

Measurements of diffusive gas exchange by air exposed sediments in darkness (diffusive S–A) was conducted in the laboratory during the dry season and in situ during the wet season. A fortunate equipment upgrade allowed in situ measurements of CO_2 release in the wet season. Appropriate tests showed no significant difference between the two approaches. No diffusive S–A uptake of O_2 was measured in the wet season due to electrode malfunction.

Triplicate sediment cores without any visible biogenic structures were taken during low tide in the dry season at the four stations with 8 cm inner diameter core liners. After return to the laboratory, the depth of sediment cores was adjusted to allow 2–3 cm of air space above the sediment surface (100–150 ml headspace). The core tubes were wrapped in aluminum foil to protect the sediment from light. The diffusive O_2 uptake was calculated from the concentration change determined with a polarographic O_2 electrode (Radiometer) inserted gas tight into the headspace for 5–10 h. Diffusive CO_2 release was subsequently measured using a flow-through system. The cores were sealed gas tight and serially connected to a peristaltic pump and a Li-Cor LI-820 infrared CO_2 analyzer. The pump pulled ambient air into the headspace of the cores at a rate of 44 ml min^{-1} (turnover time of 1–3 min) and out through the gas analyzer. CO_2 exchange was calculated as the steady state concentration difference between excurrent gas and atmospheric air.

In situ diffusive CO_2 exchange measurements in wet season were conducted using a Li-Cor LI-6400 Portable Photosynthesis System. The sensor-head of the LI-6400 was mounted on a custom made Plexiglas flux chamber (8 cm inner diameter and 18 cm long). The chamber was darkened with alu-foil and deployed by carefully pushing the open lower end about 5 cm into the upper root-free sediment. The measurement started immediately with the LI-6400 set for closed-chamber measurement while a circulation pump in the sensor head assured a homogeneous gas phase inside the chamber. Chamber CO_2 was allowed to change linearly for 5–10 min according to the net outcome of production and consumption processes within the sediment. Typically 2–3 repeated measurements were done during each deployment. Release of CO_2 was calculated from the slope of CO_2 concentration change and related to the volume and area of the chamber.

Anoxic sediment incubations

Anaerobic carbon oxidation and iron respiration were quantified in the dry season by closed jar incubations. Four sediment cores (8 cm diameter) were sampled from each of the four stations using acrylic core tubes. After sectioning (0–2, 2–4, 6–8 and 10–12 cm depth), the four sediment slices from each depth interval were pooled and homogenized. The homogeneous sediment mixtures from each depth interval ($\sim$200 ml) were transferred into eight 20-ml glass scintillation vials (jars), which were capped with no headspace, taped to prevent oxygen intrusion, and incubated in the dark at 28°C.

Two jars from each depth were sacrificed at 4–5-day intervals for determination of porewater total CO_2 and Fe^{2+} concentrations, as well as solid phase Fe(II). Porewater was extracted from the jars by centrifugation at $1000\times g$ for 10 min and filtered through GF/F filters. Subsamples for CO_2 and Fe^{2+} were handled and analyzed as described above. The sediment remaining after porewater extraction was homogenized, extracted and analyzed for reactive Fe(II) as described above. Reaction rates in jars were calculated from a linear fit of concentration changes in the time series of samples. Iron reduction (FeR) was determined as reactive Fe(II) accumulation assuming limited precipitation of iron into non-acid extractable phases (Canfield et al. 1993).

Denitrification assay

Rates of denitrification during immersion were measured in the wet season using the laboratory based ^{15}N isotope pairing technique on intact sediment

cores (Nielsen 1992). Procedures for sampling of sediment cores and laboratory incubations were similar to those applied for sediment–water exchange of O_2 and total CO_2. Five undisturbed sediment cores from each station were adjusted to ~10 cm height and placed into a seawater tank. After stabilization overnight, the denitrification assay was initiated by amending the water with $^{15}NO_3^-$ (99.2% ^{15}N, Sigma-Aldrich) to a final concentration of ~60 μM. The water phase was mixed manually to ensure homogeneous distribution of tracer. About 15 min later, the core tubes were sealed gas tight with rubber stoppers. After incubation in the dark for 3–5 h (O_2 did not change more than 20% from air saturation), sediment and water column in each core were mixed completely with a PVC rod. Duplicate 20 ml samples of the resulting slurry were transferred to gas-tight vials (12 ml Extainers, Labco), preserved with formaldehyde (100 μl, 38%) and sealed ensuring no entrapped air. ^{15}N content of N_2 was analyzed using combined gas chromatography/mass spectrometry (Robo-Prep-G1 in line with Tracermass, Europa Scientific). Denitrification rates were calculated from $^{29}N_2$ and $^{30}N_2$ production rates as described by Nielsen (1992).

Sulfate reduction assay

Sulfate reduction rates (SRR) were determined by the core-injection technique (Jørgensen 1978) in both the dry and wet season. The dry season SRR assay was limited to the upper 12 cm of the sediment, while depths down to 18–30 cm were examined in the wet season. Volumes of 2 μl radiolabeled sulfate (^{35}S–SO_4^{2-}) (70 kBq) were injected at 1-cm intervals along the depth axis of three 2.6 cm diameter cores taken from each of the four stations. The cores were incubated in the dark for 6 h at 28°C. The incubations were terminated and sulfide preserved by slicing 1- or 2-cm sediment sections directly into 50-ml plastic centrifuge tubes containing 5 or 10 ml of 20% (w/w) zinc acetate solution. Tubes were capped, vigorously shaken, and stored frozen until analysis. Sulfide was extracted from the sediment by the one-step distillation procedure of Fossing and Jørgensen (1989). Radioactivity was counted on subsamples from distillation traps with Ultima Gold scintillation cocktail in a Packard TriCarb 2000 scintillation counter. The total SSR represents the sum of the AVS (i.e. FeS and H_2S) and CRS (i.e. FeS_2 and S^0) fractions.

Statistical analysis

Differences in fluxes were tested among the four stations and between the two seasons using one-way ANOVA. Data for depth profiles of reaction rates, porewater solutes and solid phase parameters were evaluated by two-way repeated measures ANOVA. In some cases the ANOVA's were followed by a Bonferroni adjusted Fishers's Least Significant Difference test to resolve which treatment differed significantly. A significance level of $\alpha = 0.05$ was used in all tests. Data were analyzed using SAS (version 8).

Results

Diffusive sediment–water/air fluxes

The diffusive release of total CO_2 in the dark varied in an unpredictable pattern among stations, mangrove forests and seasons with rates ranging from 28 to 112 mmol m^{-2} day^{-1} (Fig. 2). However, a few significant trends are evident. Diffusive S–W release of CO_2 from inundated Mtoni sediment was consistently twice as high at station M1 than M5 and about twice as high in the wet than the dry season for both stations. The diffusive S–W release of CO_2 at both inundated Ras Dege stations was almost similar at an intermediate rate in the dry season, while R1 exhibited a significantly higher rate than at R5 in the wet season. Diffusive S–A release of CO_2 from air exposed sediment showed lower temporal and spatial variability than diffusive S–W release (Fig. 2). Only M1 in the dry season had significantly higher Diffusive S–A release than the other three stations.

The variation in diffusive O_2 uptake was considerably lower than for CO_2 release with no apparent influence of inundation (Fig. 2). O_2 uptake ranged from 25 to 65 mmol m^{-2} day^{-1} in both the dry and wet season. However, diffusive S–W uptake of O_2 was significantly lower in the impacted Mtoni than the pristine Ras Dege during the dry season, whereas M1 exhibited significantly higher rates than the other three stations in the wet season.

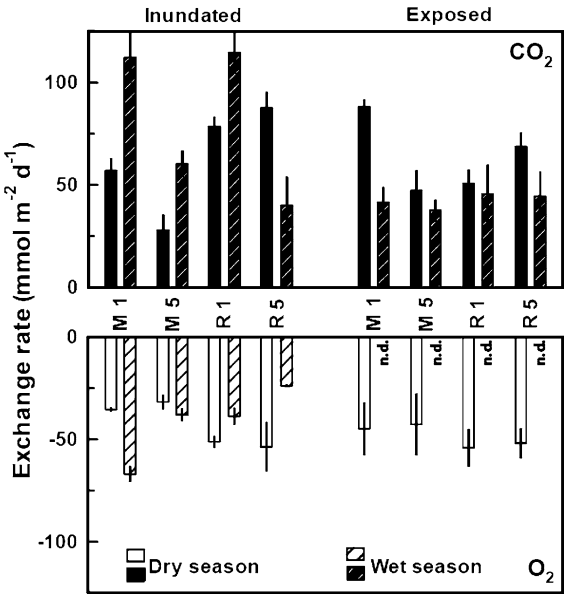

Fig. 2 Exchange of CO_2 and O_2 across the surface of sediment without large biogenic structures at the selected stations in Mtoni and Ras Dege. Measurements were made under inundated (*left*) and air exposed (*right*) conditions during the dry (not hatched) and wet (hatched) seasons. No O_2 measurements were made under exposed conditions in the wet season (marked with n.d.). Values are given as mean ± SE ($n = 3$, except for exposed wet season where $n = 6$). Positive values indicate flux out of the sediment

Anaerobic carbon oxidation pathways

Anaerobic carbon oxidation via sulfate reduction (SRR), iron reduction (FeR) and denitrification (DENITR) were determined independently, while total CO_2 production was assessed from the same anaerobic jar incubations where FeR was obtained.

SRR in the impacted Mtoni sediments was always low within the upper 12 cm with rates ranging from 5 to 50 nmol S cm^{-3} day^{-1} (Fig. 3A). M5 showed a significant seasonal pattern with SRR in the dry season about one order of magnitude higher than in the wet season. SRR at M1 in the wet season increased sharply below 12 cm depth to rates of about 220 nmol S cm^{-3} day^{-1}. No simultaneous increase was observed at M5 where the rates remained very low in the deeper sediment, reaching rates around 1 nmol S cm^{-3} day^{-1} at 30 cm depth. SRR in the pristine Ras Dege sediments showed a significant seasonal trend at R1 similar to that of M5 in Mtoni with 2–6 times higher rates in the dry than wet season (Fig. 3B). R5 exhibited significantly higher SRR than

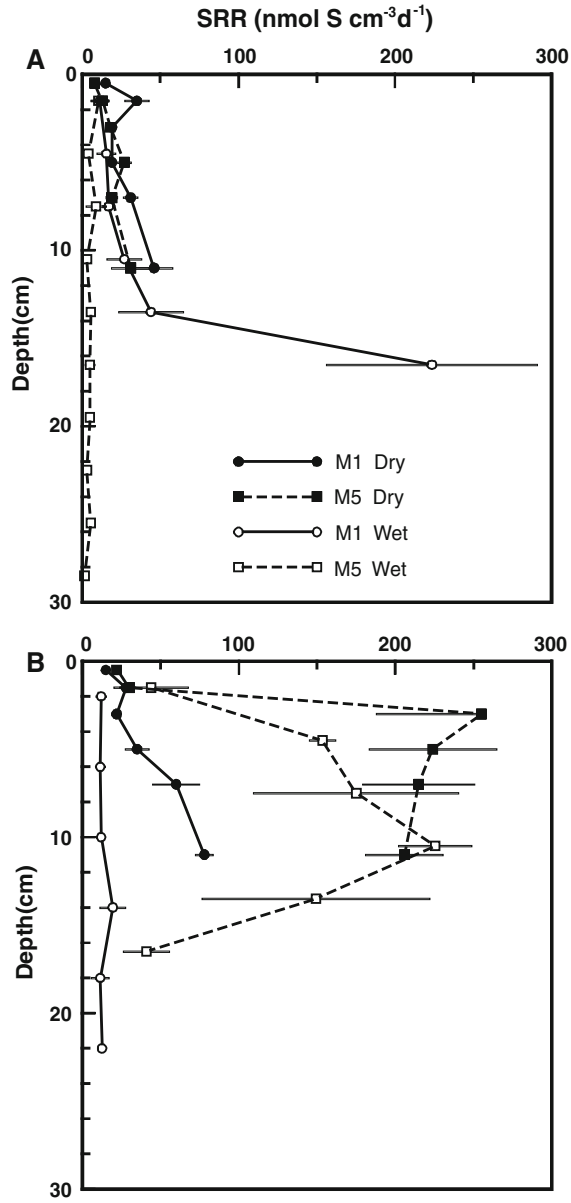

Fig. 3 Vertical profiles of sulfate reduction (SRR) in **A** Mtoni and **B** Ras Dege. Results are shown for the two stations at each location in the dry and wet season. Values are given as mean ± SE ($n = 3$)

R1 with no seasonal difference. A maximum of 150–250 nmol S cm^{-3} day^{-1} was evident from 3 to 12 cm depth with considerably lower rates above and below.

FeR was determined solely as production of solid phase Fe(II) because porewater Fe^{2+} was barely detectable and showed no temporal pattern in any of

the incubations. FeR at both Mtoni stations ranged from 0.5 to 3.5 μmol Fe cm^{-3} day^{-1} in the dry season (Fig. 4A) with highest rates in near-surface sediment and a gradual decrease below. The rates were significantly 30–150% higher at M1 than M5. FeR in Ras Dege was of the same order of magnitude as found in Mtoni, but with only insignificant depth dependent variations (Fig. 4B). The rates were significantly 35–250% higher at R1 than at R5, with largest difference in the uppermost and deepest layers.

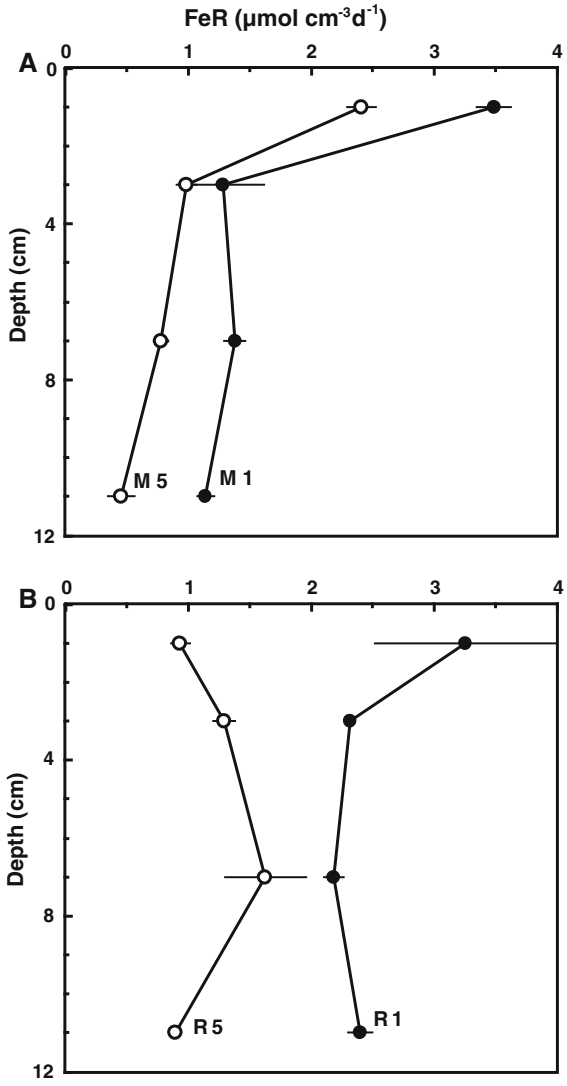

Fig. 4 Vertical profiles of iron respiration (FeR) in **A** Mtoni and **B** Ras Dege. Results are shown for the two stations at each location in the dry season. Values are given as mean ± SE ($n = 4$)

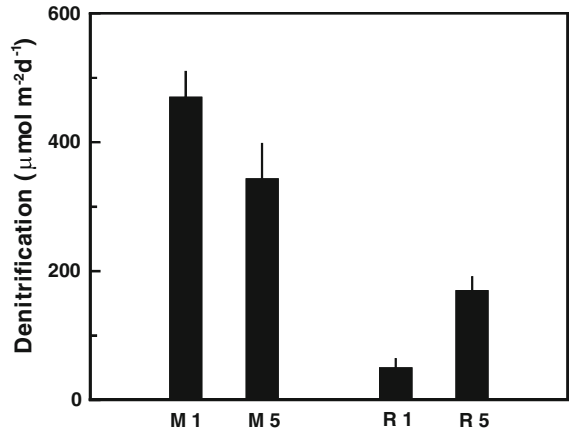

Fig. 5 Denitrification rates at Mtoni and Ras Dege determined during the wet season with the isotope pairing technique. Rates are given as mean ± SE ($n = 5$)

DENITR was generally low in both Mtoni and Ras Dege during the wet season (Fig. 5). Rates in impacted Mtoni sediment were significantly 2–10 times higher than in the pristine Ras Dege mangrove forest.

The dry season anaerobic CO_2 production in sediment from the two Mtoni stations were comparable and showed gradually decreasing rates with depth (Fig. 6A, B). The anaerobic CO_2 production in the upper 0–2 cm sediment from Ras Dege was twice as high at R1 than R5 (Fig. 6C, D). Below this depth the rates decreased significantly by 70% at R1 with only a slight increase deeper down R5 showed rates similar to those at the two Mtoni stations, but with no significant change from the surface down to 6–8 cm and an almost doubling at the deepest interval (10–12 cm).

The dry season comparison between depth profiles of measured anaerobic CO_2 production and the estimated sum of SRR, FeR and DENIT converted to carbon units (SRR × 2; FeR × 1/4; DENIT × 5/4, Kostka et al. 2002) was generally good considering the inherent uncertainty of this type of measurements (Fig. 6). The measured and estimated (FeR + SRR + DENIT) profiles of anaerobic CO_2 production generally showed similar depth patterns. The exceptions were: M1, 76% higher measured rates at 2–4 cm depth; M5, consistently 34–53% higher measured rates at all depths; R1, 100% higher measured in the 0–2 cm interval; R5, 207 and 79% higher measured than estimated rates at 0–2 and 10–12 cm depth,

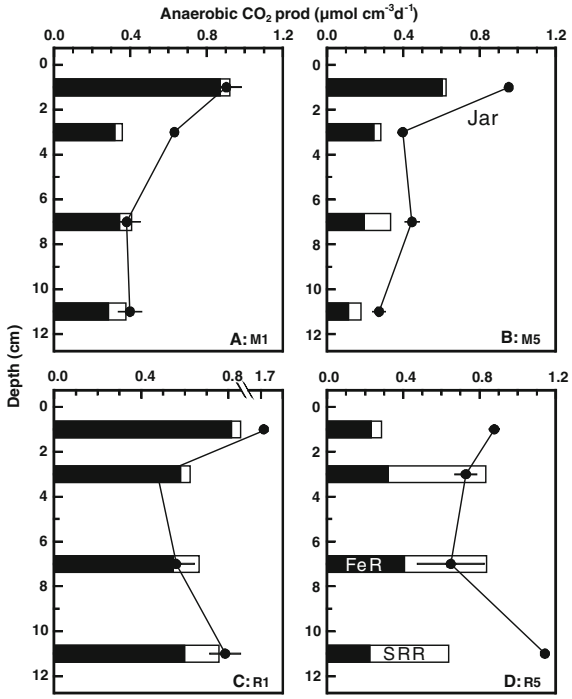

Fig. 6 Vertical profiles of anaerobic CO_2 production in **A**, **B** Mtoni and **C**, **D** Ras Dege. Results are shown for the two stations at each location in the dry season. *Symbols* and *lines* indicate total CO_2 production measured in jars. *Bars* show the sum of CO_2 produced by FeR (*solid*, from Fig. 4), SRR (*open*, from Fig. 3) and DENIT (not visible, from Fig. 5). Values are given as mean ± SE ($n = 4$). For FeR, SRR and DENIT error bars, please consult Figs. 3, 4 and 5

respectively. FeR dominated the anaerobic CO_2 production at M1, M5 and R1, while SRR dominated below 2 cm depth at R5.

Porewater profiles

The sediment water content was significantly 1.6 times higher at R5 than M1 with intermediate and similar values at M5 and R1 (Table 1). Porewater SO_4^{2-} at the two Mtoni stations was significantly lower during the wet than the dry season. The difference was most pronounced at M5 and in the upper 2 cm of the sediment at M1 (Fig. 7A, B). The sediment in Ras Dege showed porewater SO_4^{2-} similar to (R1) or higher (R5) than seawater (28 mM) during both seasons (Fig. 7C, D). Nevertheless, porewater SO_4^{2-}/Cl^- ratios were constant around 49–55 × 10^{-3} at all depths and seasons in both Mtoni and Ras Dege.

Solid phase profiles

The sediment at the two Mtoni stations had similar characteristics (Table 1). It consisted of coarse sand mixed with up to 19% silt. The organic content was low with POC around 1%. The median grain size of pristine Ras Dege sediment was less than half of impacted Mtoni sediment. It consisted of fine sand mixed with up to 38% silt. The organic content at Ras Dege was 3–5 times higher than in Mtoni; particularly at R5. The molar C:N ratio was relatively high (>25) with no significant pattern among stations. There were no significant differences in POC and PON between seasons at any station. The dry season Chl. *a* content was similar at M1, M5 and R1 at a level one order of magnitude higher than at R5 (Table 1).

Solid phase Fe differed among stations in the dry season (Fig. 8). Fe(III) generally dominated by a factor of four over Fe(II) in the upper sediment at Mtoni. Below 4–6 cm (M5) and 6–8 cm (M1), Fe(III) decreased significantly and approached the level of Fe(II). The concentration of Fe(III) at R1 was only 1.5–2 times higher than that of Fe(II) below 2 cm depth. The situation was reversed at R5, where Fe(II) exceeded Fe(III) below 1 cm depth by a factor of 1.5–6. The profiles of Fe(III) and Fe(II) at all stations generally appeared as mirror images; most pronounced at R5. Consequently, the level of total acid extractable iron (Fe(II) + Fe(III)) was remarkably constant with depth in the sediment (41–54 (M1), 27–30 (M5), 22–31 (R1) and 28–35 (R5) µmol cm^{-3}), except for M5 below 6 cm depth (down to 12 µmol cm^{-3}).

Discussion

Diffusive-based estimates of carbon oxidation

Release of CO_2 from aquatic sediments is usually considered an integrated measure of carbon oxidation by aerobic and anaerobic microbial processes occurring within the entire sediment column (Canfield et al. 2005). Accordingly, the measured diffusive release of CO_2 from inundated (diffusive S–W) and air exposed (diffusive S–A) sediments in the impacted Mtoni and pristine Ras Dege mangrove areas is remarkably similar to the estimated 0–12 cm

Table 1 Basic characteristics of sediment from the two stations in Mtoni (M) and Ras Dege (R)

	M1	M5	R1	R5
Water content (%)				
0–4 cm	28.3 ± 1.7	35.2 ± 1.2	32.7 ± 1.1	46.2 ± 4.8
4–12 cm	27.8 ± 1.8	35.0 ± 2.9	34.3 ± 0.4	44.7 ± 1.8
POC (%)				
0–4 cm	1.00 ± 0.22	1.13 ± 0.09	2.73 ± 0.05	4.84 ± 0.74
4–12 cm	1.03 ± 0.13	0.93 ± 0.18	3.07 ± 0.29	3.59 ± 0.03
PON (%)				
0–4 cm	0.050 ± 0.009	0.047 ± 0.007	0.109 ± 0.003	0.226 ± 0.032
4–12 cm	0.052 ± 0.007	0.036 ± 0.013	0.120 ± 0.016	0.160 ± 0.000
POC:PON (mol)				
0–4 cm	26.5 ± 4.7	29.7 ± 3.1	29.6 ± 0.2	23.9 ± 2.3
4–12 cm	30.3 ± 2.5	34.6 ± 9.8	30.4 ± 1.6	26.3 ± 0.1
Chl. *a* (μg g ww^{-1})				
0–1 cm	2.9 ± 1.3	2.5 ± 0.4	3.3 ± 0.9	0.4 ± 0.2
Mean grain size (mm)				
0–4 cm	0.273	0.354	0.140	0.134
4–12 cm	0.504	0.344	0.137	0.156
<63 μm fraction (%)				
0–4 cm	19.0	14.6	24.8	38.0
4–12 cm	14.3	14.7	26.4	27.1

The sediment column is split into 0–4 and 4–12 cm depth intervals, except for Chl. *a* where only data from 0 to 1 cm is shown. Values are given as combined wet and dry season means ± SD ($n = 6$,), except mean grain size ($n = 1$) and the <63 μm fraction ($n = 1$) from the dry season

depth integrated anaerobic CO_2 production (Table 2). A similar correspondence between such two independent measures has previously been observed in other mangrove environments and subtidal sediments (Canfield et al. 1993; Alongi et al. 2005).

Carbon oxidation in mangrove environments is fuelled by organic matter in the form of fresh litter and algal detritus deposited at or near the sediment surface, as well as detritus buried by accretion, by leaf-eating sesarmid crabs and by belowground root production (Alongi et al. 2005; Kristensen and Alongi 2006; Lovelock 2008). The supply and reactivity of organic carbon sources in the impacted Mtoni and pristine Ras Dege mangrove forests do not vary systematically between seasons and among sites as indicated by the inconsistent pattern and limited differences in carbon oxidation as estimated from diffusive fluxes (Fig. 2). Lack of significant seasonal and spatial changes in carbon oxidation has previously been noticed in other tropical mangrove environments (Alongi 1994; Holmer et al. 1999). These observations indicate that microbial carbon oxidation estimated from diffusive exchange of O_2 and CO_2 over the sediment–water/air interface in mangrove sediments is resilient to environmental changes.

The higher in diffusive fluxes at station M1 than M5 in the Mtoni area (Fig. 2) are probably caused by allochthonous organic input of anthropogenic origin. Drifting macroalgae transported from the shallow eutrophic area outside the mangrove forest are trapped by e.g. pneumatophores and subsequently buried into the sediment by crabs (Kristensen 2008). However, the faster degradation of the labile macroalgal detritus combined with higher tidal flushing at M1 maintains the sediment organic content low and comparable to that at M5 (Table 2) where a scattered vegetation only delivers limited amount of less reactive mangrove detritus. Similar differences in organic sources and reactivity between low and high intertidal zones have previously been observed in other mangrove forests (Alongi et al. 2000; Bouillon

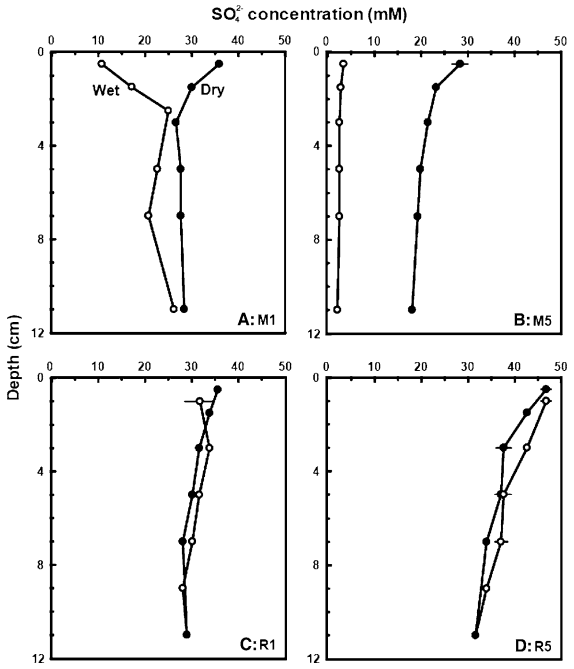

Fig. 7 Vertical profiles of porewater SO_4^{2-} in **A**, **B** Mtoni and **C**, **D** Ras Dege. Results are shown for the two stations at each location in the dry and wet season. Values are given as mean ± SE ($n = 3$)

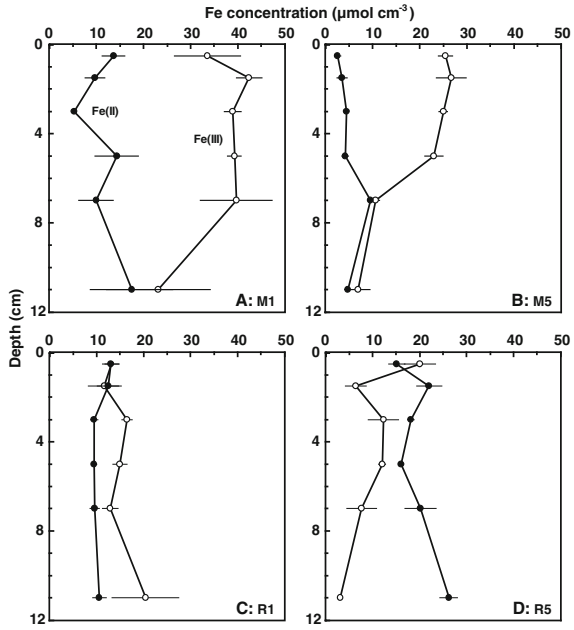

Fig. 8 Vertical profiles of solid phase iron in **A**, **B** Mtoni and **C**, **D** Ras Dege. Results are shown for the two stations at each location in the dry season. Values are given as mean ± SE ($n = 3$)

et al. 2003; Marchand et al. 2004; Poungparn et al. 2009). There is inconsistency between diffusive release of CO_2 and bulk organic content in the pristine Ras Dege sediments. The higher organic content at R5 is not reflected in the diffusive fluxes, which are comparable at the two stations (Fig. 2). The high intertidal and densely vegetated R5 is an important deposition area for relatively refractory mangrove detritus due to slow currents, while stronger currents at the low intertidal R1 prevent such deposition. The diffusive fluxes in R1 sediments are instead largely maintained by autochthonously derived microphytobenthic production. This is supported by the almost ten times higher content of Chl. *a*, and thus labile microalgal organic carbon, in surface sediment of R1 than R5. It therefore appears that near-surface heterotrophic microbial communities in low intertidal mangrove sediments are to a large extent supported by marine derived labile algal carbon sources, while high intertidal sediments primarily receives less reactive mangrove detritus.

Validity of diffusive fluxes

It is surprising that measured diffusive CO_2 release agrees well with the rather arbitrarily chosen 0–12 cm depth integrated anaerobic carbon oxidation at all study sites. The latter estimate excludes all carbon oxidation processes occurring below 12 cm in the sediments. It is evident, however, that a process like sulfate reduction is active much deeper at both Mtoni and Ras Dege (Fig. 3). In fact, the highest SRR recorded in Mtoni actually occurred at 14–16 cm depth (M1) in the wet season. Alongi et al. (2005) also found relatively high rates of sulfate reduction (100–300 nmol cm^{-3} day^{-1}) in mangrove sediments down to 1 m depth. By including sulfate reduction in these deep sediments, depth integrated rates of CO_2 production must exceed the measured diffusive S–W and S–A CO_2 release across the sediment–water interface considerably. The use of diffusive CO_2 release as a measure of total sediment carbon oxidation is therefore critical and most likely spurious in mangrove environments. Based on the present results, it appears that diffusive fluxes are representative for depth integrated carbon oxidation only in near-surface sediment to a depth of about 12 cm. All CO_2 generated deeper down must be lost by other means.

Table 2 Total benthic metabolism (mmol C m^{-2} day^{-1}) determined as diffusive dark sediment–water CO_2 release (diffusive S–W) and sediment–air CO_2 release (diffusive S–A) in the dry season

Process	M1	M5	R1	R5
CO_2 release				
Diffusive S–W	57 ± 10	28 ± 13	78 ± 8	88 ± 13
Diffusive S–A	88 ± 6	47 ± 17	51 ± 12	69 ± 12
Biogenic S–A	208 ± 58	12 ± 6	116 ± 28	43 ± 22
Daily average	177 ± 30	44 ± 11	123 ± 16	100 ± 14
Total Jar CO_2 prod	64.2 ± 3.8	57.0 ± 1.9	94.4 ± 4.9	99.6 ± 7.2
FeR CO_2 prod	49.4 ± 2.8 (77)	30.6 ± 1.3 (54)	73.5 ± 3.8 (78)	37.4 ± 3.4 (38)
SRR CO_2 prod	7.4 ± 1.5 (12)	4.9 ± 1.4 (9)	11.7 ± 2.2 (12)	45.9 ± 8.9 (46)
DENIT CO_2 prod	0.6 ± 0.1 (1.0)	0.4 ± 0.1 (0.7)	0.1 ± 0.0 (0.1)	0.2 ± 0.0 (0.2)
FeR + SRR + DENIT	57.4 ± 3.2 (89)	35.9 ± 1.9 (63)	85.3 ± 4.4 (90)	83.5 ± 9.5 (84)

The excess contribution from large biogenic structures (crab burrows and pneumatophores) at the same stations and season during air exposure (biogenic S–A) is obtained from Kristensen et al. (2008b). Total flux estimates are based on the assumption that the sediment is inundated 50% of the time. Dry season jar-rates are depth integrated from 0 to 12 cm and consist of total CO_2 production and CO_2 production from FeR. Independently measured dry season SRR and DENIT based CO_2 production are 0–12 cm depth integrated rates. Numbers in parenthesis indicate percent contribution to total jar CO_2 production

Since our measurements of diffusive CO_2 efflux were deliberately done in areas without large biogenic structures, the obtained rates do not represent the total loss of CO_2 from the sediment. Crab burrows and pneumatophores, act as conduits for CO_2 from deep sediments to the atmosphere and generate a larger total release, particularly at M1 and R1 where these structures are abundant (Table 2). Crab burrows, which are opened by their inhabitants at low tide, will augment the gas exchange by providing a much larger surface area available for diffusive transport of CO_2 to the atmosphere. Open lenticels of pneumatophores during air exposure also allow for rapid diffusion of CO_2 from deep sediments to the atmosphere via the air-filled aerenchyma tissue of roots (Purnobasuki and Suzuki 2005). Kristensen et al. (2008b) recently reported that crab burrows and pneumatophores at Mtoni and Ras Dege increase sediment–air release of CO_2 in the dark by a factor of 3.2 at M1, 1.3 at M5, 3.3 at R1 and 1.6 at R5 (Table 2). The effect of biogenic structures on CO_2 release is less pronounced during inundation because burrows are plugged by their inhabitants and lenticels of pneumatophores are closed (De la Iglesia et al. 1994; Allaway et al. 2001).

CO_2 emission via large biogenic structures does not always compensate fully for carbon oxidation occurring in deep sediments. Thus, the daily average total CO_2 efflux at M5 and R5 remains similar to or lower than the 0–12 cm integrated rates even when the contribution from large biogenic structures is included (Table 2). Another possible CO_2 sink at M5 and R5 is horizontal porewater seepage, particularly close to creeks. Thus, Bouillon et al. (2007) showed that about 30% of the creek water in Ras Dege consist of porewater during low tide slack. Accordingly, the total CO_2 in creek water more than doubled from high to low tide. Crab burrows and cavities from decaying roots are known to increase the hydraulic conductivity of mangrove sediments (Ridd 1996; Susilo et al. 2005), and thus act as channels where porewater and associated solutes can be released into creeks.

Partitioning of anaerobic carbon oxidation pathways

Heterotrophic activity in mangrove sediments is usually sufficiently fast to prevent O_2 penetration deeper than 2 mm into the sediment (Kristensen et al. 1994). The bulk sediment remains largely anoxic except for a network of infaunal burrows and roots that translocate O_2 deep into the sediment (Kristensen and Alongi 2006). O_2 is not only consumed by aerobic heterotrophs, but also by reoxidation of

reduced metabolites, such as HS^- and Fe^{2+}, diffusing to the oxic interface from the deeper anoxic sediment (Canfield et al. 2005). However, the anaerobic jar incubations used in the present study to determine partitioning of carbon oxidation pathways do not allow aerobic processes. Aerobic carbon oxidation in surface sediment due to oxygen exposure under in situ conditions is replaced by anaerobic processes in jars (i.e. FeR and SRR). Since carbon oxidation generally is slower under anoxic than oxic conditions (Kristensen and Holmer 2001), our jar rates may slightly underestimate in situ rates. The estimated (FeR + SRR + DENIT) CO_2 production is in most cases (except for M5) not significantly different from the measured anaerobic CO_2 production (Table 2). However, the trend for lower estimated than measured anaerobic CO_2 production may be due to other not accounted for processes. Thus, methanogensis accounts for <1% of carbon mineralization at the present study sites (Kristensen et al. 2008b), whereas the importance of processes such as manganese reduction and fermentation processes (Canfield et al. 2005) is currently unknown.

The contention that sulfate reduction always is the most important anaerobic respiration processes in intertidal marine sediments has recently been challenged (Kristensen et al. 2000; Kostka et al. 2002). In line with this, the present study shows that iron reduction (FeR) accounts for 38–78% of the jar-based total CO_2 production in the upper 12 cm of both impacted Mtoni and pristine Ras Dege sediment compared with 9–46% for SRR (Table 2). As sulfate reduction usually is hampered in the presence of more potent electron acceptors (e.g. O_2 and Fe(III); Canfield et al. 2005), this process becomes less important than iron respiration when oxidizing roots and infaunal burrows increase the Fe(III) content (Nielsen et al. 2003). The proportion of anaerobic respiration in mangrove sediments mediated by FeR is significantly related to the concentration of reactive oxidized iron (Fe(III)) within the sediment (Fig. 9) according to the equation of Jensen et al. (2003):

$$\%\mathrm{FeR} = 100\left(1 - e^{-a[\mathrm{Fe(III)}]}\right) \quad (1)$$

where $a = 0.053 \pm 0.006$ for four different mangrove sediments from three continents. The relationship shows that more than 80% of the anaerobic carbon oxidation in mangrove sediments is due to microbial FeR when the concentration of reactive Fe(III) exceeds about 30 μmol cm^{-3}. This is similar to that found for a number of coastal marine areas in temperate regions (dashed line in Fig. 9, $a = 0.056 \pm 0.004$; Jensen et al. 2003) and points towards a universal relationship for marine sediments. A similar relationship, but with lower a (0.029 ± 0.002), is evident from the data obtained by Roden and Wetzel (2002) for freshwater wetlands (dotted line in Fig. 9).

The similarity in partitioning of carbon oxidation pathways and dominance of FeR in the upper 12 cm of the low intertidal stations (M1 and R1): 77–78% FeR; 12% SRR; and 0.1–1% denitrification (Table 2), are probably associated with the oxidizing effect of the numerous pneumatophores and crab burrows in the iron-rich muddy sand. Particularly tree species with numerous pneumatophores and a dense network of near-surface roots (e.g. *A. marina*) have capacity to oxidize the sediment and thus hamper SRR (Alongi et al. 2000; Kristensen and Alongi 2006). Also crab burrows are known as reinforcers of FeR decimeters into the sediment (Clark et al. 1998; Nielsen et al. 2003). Thus, organic enrichment of anthropogenic

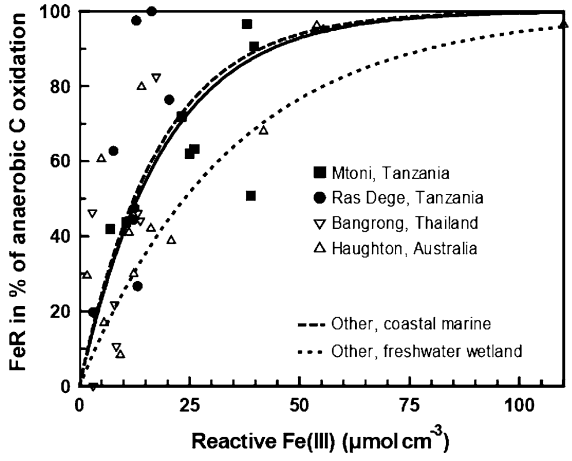

Fig. 9 Relationship between the concentration of reactive Fe(III) and the proportion of iron respiration (FeR) of total anaerobic carbon oxidation in mangrove sediments from Mtoni and Ras Dege, Tanzania (this study); Bangrong, Thailand (Kristensen et al. 2000); and Haughton, Australia (Kristensen and Alongi 2006). *Full line* shows the best fit to the data from mangrove environments using Eq. 1) with a constant $a = 0.053$. The *broken line* shows the general relationship found for non-mangrove coastal marine areas with $a = 0.056$ as reported by Jensen et al. (2003). The *dotted line* represents the relationship with $a = 0.029$ for a freshwater wetland located in the Talladega National Forest, Alabama, USA (Roden and Wetzel 2002)

origin, which is usually known to promote SRR in marine sediments (Berelson et al. 2002), has no obvious influence on the partitioning of FeR and SRR at M1 when compared with R1. Biogenic structures have apparently sufficient oxidizing capacity to prevent sulfidic conditions.

FeR is less important for carbon oxidation at the high intertidal stations (M5: 54%; R5: 38%), while SRR account for as much as 46% at R5 but only 9% at M5 (Table 2). The high sulfate reduction in the 1–10 cm sediment layer of the fine grained and organic-rich sediment at R5 vegetated by *R. mucronata* is conspicuous. Alongi et al. (2000) similarly reported that sulfate reduction is responsible for ~2.5 times higher fraction of sedimentary carbon oxidation in dense *Rhizophora* forests than more open *Avicennia* forests in Western Australian. The impermeable nature of silty sediments and the limited oxidation capacity of *R. mucronata* roots allow only limited reoxidation of iron and sulfide (Marchand et al. 2004). Much of the generated sulfide is probably precipitated by the available pool of reduced iron (Fig. 8). The low SRR at M5, is puzzling when the almost absence of pneumatophores and burrows is considered. Since the discrepancy between estimated (FeR + SRR + DENIT) and measured anaerobic jar CO_2 production is most pronounced at this station (Table 2), unaccounted processes may have had a significant role. In accordance, Kristensen et al. (2008b) observed four times higher CH_4 release from M5 than M1 during the dry season. Methanogenesis may be particularly important at M5 during the wet season when sulfate reduction is hampered by depletion of porewater SO_4^{2-} (Fig. 7).

Denitrification is usually low in mangrove sediments due to inorganic nitrogen limitation (Rivera-Monroy and Twilley 1996; Lee and Joye 2006), and only mangrove environments impacted by wastewater rich in NO_3^- support high rates of denitrification (Corredor and Morell 1994; Alongi et al. 1999). Mtoni and Ras Dege follow these trends since less than 1% of the total carbon oxidation is supported by denitrification (Table 2). The anthropogenic impact at Mtoni (loading of ~3 mol N m^{-2} $year^{-1}$, M.R. Flindt, unpublished) maintains NO_3^- at a higher level (5–20 μM) than in the pristine Ras Dege area (loading of ~0.1 mol N m^{-2} $year^{-1}$, M.R. Flindt, unpublished) where NO_3^- is rarely detectable (0–2 μM; Mangion, in prep.). As a consequence, denitrification is up to one order of magnitude higher in impacted Mtoni than pristine Ras Dege sediments (Fig. 5).

Conclusions

Microbial carbon oxidation determined as diffusive release of CO_2 appears unaffected by tidal and seasonal variations in both the impacted Mtoni and the pristine Ras Dege mangrove forest. Low intertidal sediments are to a large extent supported by marine derived labile algal carbon sources, while high intertidal sediments primarily receives less reactive mangrove detritus. The diffusive exchange of O_2 and CO_2 remains similar, unless the system or parts of it is affected by organic input of anthropogenic origin. The excess organic input is counteracted by faster carbon oxidation and maintains the inventory of organic carbon at a low level. However, diffusive release of CO_2 is not an appropriate measure of total sediment carbon oxidation because substantial amounts of CO_2 are lost via emission through biogenic structures and porewater seepage into creeks. It appears that diffusive fluxes are representative for near-surface sediment to a depth of only about 12 cm. Anaerobic carbon oxidation is dominated by FeR in sediments with high abundance of biogenic structures, irrespective of anthropogenic influence. Thus, the importance of FeR is controlled by concentration of oxidized iron within the sediment, which in turn is controlled by the oxidizing capacity of mangrove roots and crab burrows. It is remarkable, though, that organic and nutrient enrichment of anthropogenic origin in Mtoni has no measurable effect on microbial processes, other than carbon oxidation in the low intertidal area and denitrification throughout the forest, and points to a strong resilience of mangrove environments towards disturbances.

Acknowledgements We are grateful for invaluable help in the field by Mads Grue and Morten S. Andersen. Our gratitude is also due to Birthe Christensen for skilful technical assistance. This research was supported by the EC-INCO programme PUMPSEA (contract 510863), The Carlsberg Foundation (contract 2005-1-325) and the Danish Research Agency (contract 09-071369).

References

Allaway WG, Curran M, Hollington LM, Ricketts MC, Skelton NJ (2001) Gas space and oxygen exchange in roots of *Avicennia marina* (Forssk.) Vierh. var. *australasica* (Walp.) Moldenke ex N. C. Duke, the Grey Mangrove. Wetl Ecol Manag 9:211–218

Alongi DM (1994) Zonation and seasonality of benthic primary production and community respiration in tropical mangrove forests. Oecologia 98:320–327

Alongi DM, Tirendi F, Dixon P, Trott LA, Brunskill GJ (1999) Mineralization of organic matter in intertidal sediments of a tropical semi-enclosed delta. Estuar Coast Shelf Sci 48:451–467

Alongi DM, Tirendi F, Clough BF (2000) Below-ground decomposition of organic matter in forests of the mangroves *Rhizophora stylosa* and *Avicennia marina* along the arid coast of Western Australia. Aquat Bot 68: 97–122

Alongi DM, Sasekumar A, Chong CV, Pfizner J, Trott LA, Tirendi F, Dixon P, Brunskill GJ (2004) Sediment accumulation and organic material flux in a managed mangrove ecosystem: estimates of land-ocean-atmosphere exchange in peninsular Malaysia. Mar Geol 208:383–402

Alongi DM, Pfitzner J, Trott LA, Tirendi F, Dixon P, Klumpp DW (2005) Rapid sediment accumulation and microbial mineralization in forests of the mangrove *Kandelia candel* in the Jiulongliang Estuary, China. Estuar Coast Shelf Sci 63:605–618

Alongi DM, Trott LA, Rachmansyah, Tirendi F, McKinnon AD, Undu MC (2008) Growth and development of mangrove forests overlying smothered coral reefs, Sulawesi and Sumatra, Indonesia. Mar Ecol Prog Ser 370:97–109

Berelson WM, Johnson K, Coale K, Li HC (2002) Organic matter diagenesis in the sediments of the San Pedro Shelf along a transect affected by sewage effluent. Cont Shelf Res 22:1101–1115

Borges AV, Djenidi S, Lacroix G, Theate J, Delille B, Frankignoulle M (2003) Atmospheric CO_2 flux from mangrove surrounding waters. Geophys Res Lett 30:1558. doi:10.1029/2003GL017143

Bouillon S, Dahdouh-Guebas F, Rao AVVS, Koedam N, Dehairs F (2003) Sources of organic carbon in mangrove sediments: variability and possible ecological implications. Hydrobiologia 495:33–39

Bouillon S, Middelburg JJ, Dehairs F, Borges AV, Abril G, Flindt MR, Ulomi S, Kristensen E (2007) Importance of intertidal sediment processes and porewater exchange on the water column biogeochemistry in a pristine mangrove creek (Ras Dege, Tanzania). Biogeosciences 4:311–322

Bouillon S, Borges AV, Castañeda-Moya E, Diele K, Dittmar T, Duke NC, Kristensen E, Lee SY, Marchand C, Middelburg JJ, Rivera-Monroy VH, Smith TJ III, Twilley RR (2008) Mangrove production and carbon sinks: a revision of global budget estimates. Global Biogeochem Cycles 22:GB2013. doi:10.1029/2007GB003052

Canfield DE, Thamdrup B, Hansen JW (1993) The anaerobic degradation of organic matter in Danish coastal sediments: iron reduction, manganese reduction, and sulfate reduction. Geochim Cosmochim Acta 57:3867–3883

Canfield DE, Kristensen E, Thamdrup B (2005) Aquatic geomicrobiology. Elsevier, Amsterdam

Clark MW, McConchie D, Lewis DW, Saenger P (1998) Redox stratification and heavy metal partitioning in *Avicennia*-dominated mangrove sediments: a geochemical model. Chem Geol 149:147–171

Corredor JE, Morell JM (1994) Nitrate depuration of secondary sewage effluents in mangrove sediments. Estuaries 17:295–300

De la Iglesia HO, Rodriquez EM, Dezi RE (1994) Burrow plugging in the crab *Uca uruguayensis* and its synchronization with photoperiod and tides. Physiol Behav 55:913–919

Dittmar T, Hertkorn N, Kattner G, Lara RJ (2006) Mangroves, a major source of dissolved organic carbon to the oceans. Glob Biogeochem Cycles 20:GB1012. doi:10.1029/2005GB002570

Ferreira TO, Otero XL, Vidal-Torrado P, Macías F (2007) Effects of bioturbation by root and crab activity on iron and sulfur biogeochemistry in mangrove substrate. Geoderma 142:36–46

Fossing H, Jørgensen BB (1989) Measurement of bacterial sulfate-reduction in sediments: evaluation of a single-step chromium reduction method. Biogeochemistry 8:205–222

Granek E, Ruttenberg BI (2008) Changes in biotic and abiotic processes following mangrove clearing. Estuar Coast Shelf Sci 80:555–562

Hall POJ, Aller RC (1992) Rapid, small-volume flow injection analysis for ΣCO_2 and NH_4^+ in marine and freshwaters. Limnol Oceanogr 37:1113–1118

Holmer M, Andersen FØ, Holmboe N, Kristensen E, Thongtham N (1999) Transformation and exchange processes in the Bangrong mangrove forest-seagrass bed system, Thailand. Seasonal and spatial variations in benthic metabolism and sulfur biogeochemistry. Aquat Microb Ecol 20:203–212

Jennerjahn TC, Ittekkot V (2002) Relevance of mangroves for the production and deposition of organic matter along tropical continental margins. Naturwissenschaften 89: 23–30

Jensen MM, Thamdrup B, Rysgaard S, Holmer M, Fossing H (2003) Rates and regulation of microbial iron reduction in sediments of the Baltic-North Sea transition. Biogeochemistry 65:295–317

Jørgensen BB (1978) A comparison of methods for the quantification of bacterial sulfate reduction in coastal marine sediments. Geomicrobiol J 1:11–27

Kitaya Y, Yabuki K, Kiyota M, Tani A, Hirano T, Aiga I (2002) Gas exchange and oxygen concentration in pneumatophores and prop roots of four mangrove species. Trees 16:155–158

Kostka JE, Luther GW (1994) Partitioning and speciation of solid phase iron in saltmarsh sediments. Geochim Cosmochim Acta 58:1701–1710

Kostka JE, Gribsholt B, Petrie E, Dalton D, Skelton H, Kristensen E (2002) The rates and pathways of carbon oxidation in bioturbated saltmarsh sediments. Limnol Oceanogr 47:230–240

Kristensen E (2008) Mangrove crabs as ecosystem engineers; with emphasis on sediment processes. J Sea Res 59:30–43

Kristensen E, Alongi DM (2006) Control by fiddler crabs (*Uca vocans*) and plant roots (*Avicennia marina*) on carbon, iron and sulfur biogeochemistry in mangrove sediment. Limnol Oceanogr 51:1557–1571

Kristensen E, Andersen FØ (1987) Determination of organic carbon in marine sediments: comparison of two CHN-analyzer methods. J Exp Mar Biol Ecol 109:15–23

Kristensen E, Holmer M (2001) Decomposition of plant materials in marine sediment exposed to different electron acceptors (O_2, NO_3^- and SO_4^{2-}), with emphasis on substrate origin, degradation kinetics and the role of bioturbation. Geochim Cosmochim Acta 65:419–434

Kristensen E, King GM, Banta GT, Holmer M, Jensen MH, Hansen K, Bussarawit N (1994) Acetate turnover, sulfate reduction and carbon metabolism in sediments of the Ao Nam Bor mangrove, Phuket, Thailand. Mar Ecol Prog Ser 109:245–255

Kristensen E, Andersen FØ, Holmboe N, Holmer M, Thongtham N (2000) Carbon and nitrogen mineralization in sediment of the Bangrong mangrove area, Phuket, Thailand. Aquat Microb Ecol 22:199–213

Kristensen E, Bouillon S, Dittmar T, Marchand C (2008a) Organic carbon dynamics in mangrove ecosystems. Aquat Bot 89:201–219

Kristensen E, Flindt MR, Borges AV, Bouillon S (2008b) Emission of CO_2 and CH_4 to the atmosphere by sediments and open waters in two Tanzanian mangrove forests. Mar Ecol Prog Ser 370:53–67

Lee RY, Joye SB (2006) Seasonal patterns of nitrogen fixation and denitrification in oceanic mangrove habitats. Mar Ecol Prog Ser 307:127–141

Lovelock CE (2008) Soil respiration and belowground carbon allocation in mangrove forests. Ecosystems 11:342–354

Lovley DR, Phillips EJP (1987) Rapid assay for microbially reducible ferric iron in aquatic sediments. Appl Environ Microbiol 53:1536–1540

Marchand C, Baltzer F, Lallier-Verges E, Alberic P (2004) Pore-water chemistry in mangrove sediments: relationship with species composition and developmental stages (French Guiana). Mar Geol 208:361–381

Middelburg JJ, Nieuwenhuize J, Slim FJ, Ohowa B (1996) Sediment biogeochemistry in an East African mangrove forest (Gazi Bay, Kenya). Biogeochemistry 34:133–155

Nielsen LP (1992) Denitrification in sediment determined from isotope pairing. FEMS Microbiol Ecol 86:357–362

Nielsen OI, Kristensen E, Macintosh DJ (2003) Impact of fiddler crabs (*Uca* spp) on rates and pathways of benthic mineralization in deposited shrimp pond waste. J Exp Mar Biol Ecol 289:59–81

Parsons TR, Maita Y, Lalli CM (1984) A manual of chemical and biological methods for seawater analysis. Pergamon Press, Oxford

Penha-Lopes G, Bartolini F, Limbu S, Cannicci S, Kristensen E, Paula J (2009) Are fiddler crabs potentially useful ecosystem engineers in mangrove wastewater wetlands? Mar Pollut Bull 58:1694–1703

Poungparn S, Komiyama A, Tanaka A, Sangtiean T, Maknual C, Kato S, Tanapermpool P, Patanaponpaiboon P (2009) Carbon dioxide emission through soil respiration in a secondary mangrove forest of eastern Thailand. J Trop Ecol 25:393–400

Purnobasuki H, Suzuki M (2005) Aerenchyma tissue development and gas-pathway structure in root of *Avicennia marina* (Forsk.) Vierh. J Plant Res 118:285–294

Ridd PV (1996) Flow through animal burrows in mangrove creeks. Estuar Coast Shelf Sci 43:617–625

Rivera-Monroy VH, Twilley RR (1996) The relative role of denitrification and immobilization in the fate of inorganic nitrogen in mangrove sediments (Terminos Lagoon, Mexico). Limnol Oceanogr 41:284–296

Roden EE, Wetzel RG (2002) Kinetics of microbial Fe(III) oxide reduction in freshwater wetland sediments. Limnol Oceanogr 47:198–211

Susilo A, Ridd PV, Thomas S (2005) Comparison between tidally driven groundwater flow and flushing of animal burrows in tropical mangrove swamps. Wetl Ecol Manag 13:377–388